

Seed dependence of the anti-correlations between the default-mode network and task-positive network

Jingyuan Chen¹ and Gary Glover¹

¹Stanford University, Stanford, CA, United States

Target Audience: fMRI researchers, or neuroscientists interested in brain resting-state connectivity

Introduction: With seed-based correlation analysis, literatures on brain spontaneous activity have demonstrated that the default-mode network (DMN) is negatively correlated with a set of brain regions, referred to as the task-positive network (TPN) at rest^[1]. However, regions compromised in the TPN and the extent of anti-correlations are inconsistent across different studies. It's widely acknowledged that the reported inconsistency derives from specific MR acquisitions and distinct preprocessing steps^[2,3,4]: studies without correcting for physiological noise may fail to unveil anti-correlations buried in the physiological noises; while those conducting global signal regression (GSR) may demonstrate spurious anti-correlations due to the improper removal of informative neural information. Recently, it has been shown that posterior cingulate cortex (PCC), the typical seed adopted by conventional analysis to study functional connectivity with respect to the DMN, has heterogeneous functions within its subparts^[5]. It's likely that seeds residing in different functional units may lead to discrepant positive/negative correlation patterns, which has never been addressed in prior studies. Here, we first obtained different PCC seeds via parcellation, then employed conventional correlation analysis and recently proposed point-process analysis^[6] to study such seed dependences of the observed anti-correlations between the DMN and TPN.

Methods: 20 healthy subjects participated in the study; each underwent an 8-min resting-state scan (relaxed & closed eyes). fMRI Images were acquired at 3T (GE Signa 750, spiral-in/out sequence^[7], TR=2s). Respiration and cardiac (pulse oximetry) data were recorded using the scanner's built-in physiological monitoring system. A bite-bar was used to inhibit significant subject motion. Common preprocessing consisted of slice time correction, detrending and nuisance regression (six head motion parameters, signals from the white matter and the CSF). **PCC seeds selection** (further preprocessing included model-based physiological noise correction^[8,9], normalization to the MNI template (2*2*2 mm³)): (1) Voxels in a pre-selected anatomical region (including left/right PCC/precuneus from AAL atlas, ~7500 voxels) were classified into multiple clusters based on their person correlations with the rest regions of the brain; (2) Cluster number varied from 2 to 8 in the analysis, the PCC parcellation result corresponding to 4 is reported here. Centroids of two clustered PCC subparts were adopted for later analysis (Figure 1). **Seed-based correlation analysis** (further preprocessing included spatial smoothing (FWHM = 4mm)): positive/negative Pearson correlation maps with respect to two PCC seeds were calculated and compared across datasets on which the following preprocesses were further performed: (1) no correction ('none'); (2) model-based physiological noise correction ('phys'); (3) global signal regression ('gsr'). Analysis was first conducted in subjects' native spaces, the generated correlation maps were normalized to the MNI template for group comparisons. **Point-process analysis** (further preprocessing included model-based physiological noise correction, spatial smoothing (FWHM = 4mm)): Recently, it has been shown that the connectivity patterns revealed by correlation analysis could be replicated by averaging a few critical points, such point-process-analysis allows us to explore deeper into the activation patterns associated with different seeds: (1) Time points with seed signal intensity amongst the top 30% were selected to reflect the 'activation events' associated with PCC1/PCC2 separately; (2) Selected time points were further grouped into three categories: 'PCC1 events + PCC2 events', 'PCC1 events + PCC2 events', 'PCC1 events + PCC2 events'. (3) Time points were averaged within each group for further comparisons.

Results & Discussions:

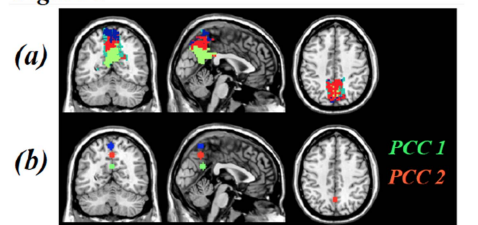
- PCC seeds selection** The parcellated PCC regions didn't match the dorsal/ventral parts reported by previous literature^[5] very well, we therefore referred to the two chosen seeds as PCC1/PCC2 instead of ventral/dorsal PCC seeds. However, positive correlations with respect to the two seeds exhibited remarkable similarity with the dorsal/ventral DMN templates published by Stanford Find lab (Figure 2).
- Anti-correlations between DMN vs TPN** Consistent with previous literatures, different preprocessing steps could alter connectivity patterns in significant manners (Figure 3, different rows). Taking 'phys' datasets as the ground truth, we observed salient seed-dependence of the anti-correlations between the DMN and the TPN: typical regions (insula, DLPFC, SMG) were present in regions negatively correlated with PCC1, while no regions showed up in the map of PCC2. Notably, the anti-correlated regions were well preserved even without any physiological signal correction ($t < -4.5$, FDR $p < 0.05$). Also, as pointed out by previous studies, global signal regression resulted in broadened anti-correlations between DMN and TPN (even with respect to PCC2), and diminished positive correlations within the DMN.
- Activation patterns associated with different PCC seeds.** Frame averages indicated significantly distinct spatial patterns under cases when PCC1 and PCC2 signals exhibited different intensity patterns (Figure 4), further demonstrating different network patterns associated with distinct PCC seeds, and highlighting the importance of seed selection in exploring dynamic interplays between the DMN and TPN in resting-state analysis.

Conclusions:

In the present study, both conventional correlation analysis and point process analysis demonstrated significant seed-dependence of the anti-correlations between the DMN and TPN.

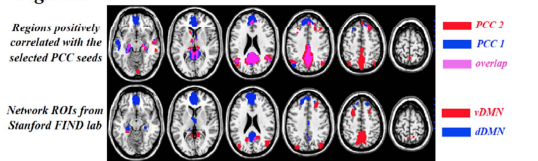
Acknowledgements: Funding support was provided by NIH P41 EB15891. **References:** [1] Fox et al., PNAS 2005; [2] Murphy et al., NI, 2009; [3] Saad et al., Brain Connectivity, 2012; [4] Chang et al., NI, 2009; [5] Leech et al., Brain, 2013; [6] Liu et al., PNAS, 2013; [7] Glover & Law, MRM 2001; [8] Glover et al., 2000; [9] Chang et al., NI 2009

Figure 1



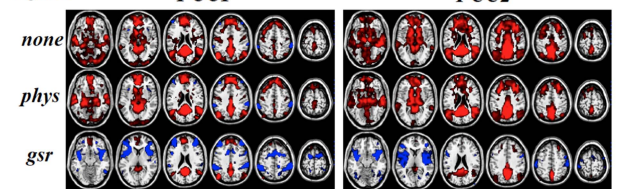
PCC parcellation results (a), centroids as PCC seeds (b)

Figure 2



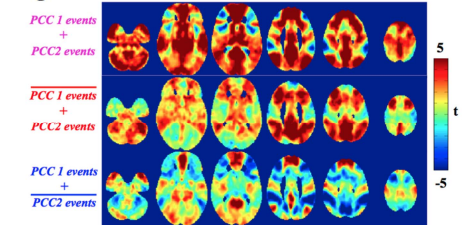
Comparisons between PCC1/PCC2-correlation maps and vDMN/dDMN templates

Figure 3



Group t scores of correlation maps with respect to PCC seeds using datasets after different preprocessing steps

Figure 4



Group t map of frame averages under three conditions